Growth of β-Ga_2O_3 nanowires via CVD using Au catalyst

Author: Anna Bertomeu i Baldé
Advisor: Albert Romano Rodríguez
Facultat de Física, Universitat de Barcelona, Diagonal 645, 08028 Barcelona, Spain.*

Abstract: Monoclinic gallium oxide nanowires have been synthesised on a silicon substrate by chemical vapor deposition using metal gallium as a precursor, argon as a carrier gas and gold as a catalyst. The effect of the separation distance between metal source and substrate, growth temperature, gas flow rate, duration of the growth and the catalyst role have been studied using several characterization techniques.

I. INTRODUCTION

Gallium oxide (Ga_2O_3) is a technologically promising semiconductor material since it is synthesizable at the nano scale and can crystalize in several polymorphic forms. The most interesting phases are the rhombohedral (α) and the monoclinic (β) [1]. Specially β-Ga_2O_3 has received considerable interest due to its outstanding properties such as wide bandgap (~4.8 eV), high breakdown field strength (8 MV/cm), thermal and chemical stability [2]. This is the reason why this material has several potential applications such as power electronics, solar-blind photodetectors and gas sensors.

The controllable growth of one-dimensional β-Ga_2O_3 nanowires (NWs) is interesting because it would open up new possibilities and opportunities in the scaling down to achieve ultracompact nanoscale electronic devices [3]. To synthesize the NWs, different methods can be employed such as the vapor-liquid-solid (VLS) mechanism. It consists of introducing a catalyst which forms a liquid alloy phase with the substrate and can rapidly adsorb a vapor to supersaturation levels, and from which crystal growth can then occur from nucleated seeds at the liquid–solid interface [4]. VLS can be carried out by different techniques: chemical vapor deposition (CVD), laser ablation (LA) or molecular beam epitaxy (MBE). Even though it is hard to achieve a proper control by CVD, it is considerably cheaper and simpler in comparison to the other techniques [4].

From the wide range of applications that this material has, our group is focused on the fabrication of gas sensors based on individual metal oxide (MOX) nanowires [5]. Since published papers related to the use of β-Ga_2O_3 nanowires as sensors are still scarce, the group has been testing gas sensors based on individual Ga_2O_3 nanowires, among others. These, which were synthesised using the oxide powder-source mixed with graphite, proved to be candidates for room temperature humidity gas sensors [6].

In this study, the possibility of growing β-Ga_2O_3 nanowires by CVD technique using gallium metal as a precursor has been explored, employing various experimental conditions. The resulting nanowires have been characterized using scanning electron microscopy (SEM), X-ray diffraction (XRD), transmission electron microscopy (TEM) and ultraviolet-visible (UV-VIS) spectrophotometry.

II. EXPERIMENTAL

A. Synthesis of Ga_2O_3 nanowires

Crystalline Ga_2O_3 NWs have been grown via the VLS mechanism using a CVD furnace connected to a rotary vane pump and a gas injection system formed by 4 MKS Mass-Flow controllers.

The synthesis was carried out in a 5 cm diameter quartz tube inserted into a Lindbergh furnace, so that the precursor and the substrates were kept at the same temperature. The precursor was put on a boat and located adjacent to the gas injection system. On either side of the precursor, a set of substrates were placed on specific positions between 0.2 and 18 cm from the evaporating source. The exact experimental layout is shown in Fig. 1.

For each experiment, the precursor material has been 0.25 ± 0.01 g of gallium metal (99.99% trace metal basis, Aldrich). To transport the precursor along the tube once it is evaporated, pure argon (5N quality) has been injected through the Mass-Flow controllers. The substrates were 0.5 × 0.5 cm^2 pieces cut from a 4-inch thermally oxidized Si wafer, with a 0.5 µm-thick SiO_2 layer. These substrates were first cleaned with acetone and then isopropanol, during 5 min each in a clean room, and next, they were dried with a N_2 blow gun. Afterwards, the substrates were Au sputter-covered for 20 s to provide the catalyst to support the VLS growth.

Before starting the experiment, the furnace tube was evacuated by the rotary vane pump to reduce eventual water vapour in the tube. Then, the system, controlled through the Atomate Workbench software, was launched and the gas flow automatically started. The pressure was maintained at ~800 Torr throughout the experiments.

Different parameters, which could influence the CVD growth, have been explored. The first experiment done was used as a reference for the rest of the experiments.

For the reference experiment, the furnace was heated at a rate of 1.5°C/min until 900°C was reached and kept at this temperature for 60 min. Then, the furnace was allowed to naturally cool down. An Ar flow rate of 100 sccm was used during the heating and the cooling phases, whereas a 2000 sccm rate was used during the deposition step. The rest of the experiments were performed in the same way but changing the

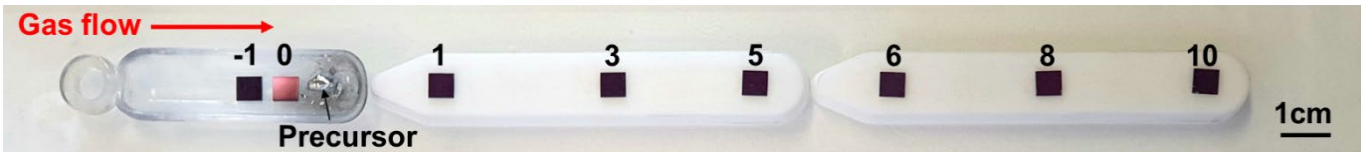

FIG. 1: Image of the experimental layout inside the quartz tube. It shows 8 labelled positions which are the typical studied in this work.

* Electronic address: abertoib7@alumnes.ub.edu

conditions: the temperature was varied between 800 and 900°C; the duration of the growth between 1 and 5 h; and the Ar flow rate during the deposition step, between 100 and 2000 sccm.

B. Characterization

The morphology of the NWs was investigated using SEM (JSM-7001F, JEOL) operated at 5.0 kV without the need of sputter-cover the samples to prevent charging.

The structure of the NWs was investigated with an X-Ray Diffractometer (X'Pert PRO MRD, PANalytical) using Cu K_α (λ = 0.1541874 nm) radiation in grazing incidence configuration, with an incidence angle of 1° to the surface.

The detailed microstructure of some of the NWs was analysed using TEM (JEM 2010F 200 kV, JEOL) equipped with an electron energy loss spectrometer (EELS), which was used to detect the elements of the NWs. To carry out the TEM analysis, the NWs were transferred to a holey carbon grid by immersing the substrate in a vial with few millilitres of toluene, sonicating for 10 s to promote their detachment from the growth substrate's surface and depositing one droplet of solution (0.5 µl) onto the grid.

Finally, an UV–VIS spectrophotometer (Specord 205, Analytik Jena) was used to investigate the optical properties of the Ga_2O_3 NWs. For this, the NWs were grown on a fused silica substrate to avoid light absorption that occurs in silicon.

III. RESULTS AND DISCUSSION

A. Morphological characterization

The SEM images of the reference experiment show a dense layer of NWs, which covers the whole substrate. This is true for all the samples mentioned in Fig. 1, even in the −1 and 0 positions that are on the left side (upstream) of the precursor. This indicates that, when the gallium evaporated, some molecules reached the mentioned samples even though the Ar gas was flowing and transporting Ga in the opposite direction. Probably this is due to some turbulence around the precursor boat.

Moreover, images (not shown here) proved that the dimensions of the NWs decrease with distance. This result is coherent since it is well known that reactant species are consumed while flowing downstream in CVD processes [7]. Consequently, the positions -1, 0 and 1, which are the closest to the precursor, present the longest NWs, of up to several micrometres. The SEM images in Fig. 2 prove the growth of NWs at the sample farthest away from the precursor.

Since the nanowires in Fig. 2b clearly show a Au particle at their tip, this confirms that the NWs were grown via VLS mechanism.

On the other hand, a comparative study of nanowires grown under different conditions has been carried out by analysing the samples of different experiments.

Previous studies suggested that the appropriate growth temperatures of Ga_2O_3 NWs using gallium metal source is in the temperature range of 700–900°C and that similar diameter and surface morphology are obtained [8]. However, in this work, the dimensions of the resulting nanowires grown at 900°C versus those grown at 800°C are quite different: NWs dimensions are shorter at 800°C. This is illustrated in Fig. 3a and Fig. 3b respectively. That is because in both experiments the amount of precursor used and the duration of the growth were the same, whereas the vapor pressure of the Ga is ~0.09 Pa at 900°C and ~0.009 Pa at 800°C [9]. Thus, less gallium was evaporated at the lower temperature, so that the amount was not enough to grow large nanowires. This fact suggests that the growth temperature is a relevant parameter that can affect the morphology. Wagner, and later Givargizov, already gave large evidence that the growth temperature determines the growth rate, diameter and stability of the nanowires [10,11].

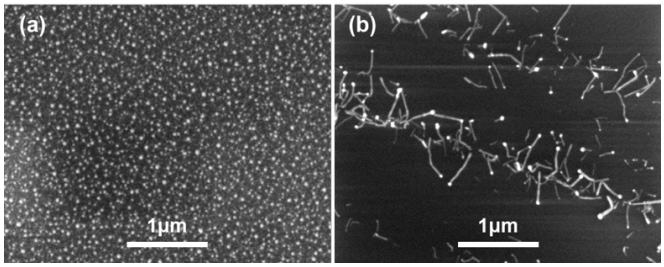

FIG. 2: SEM images of the same sample located at ~18 cm from the precursor. (a) Region with denser growth of Ga_2O_3. (b) Image of a hole on the layer of NWs.

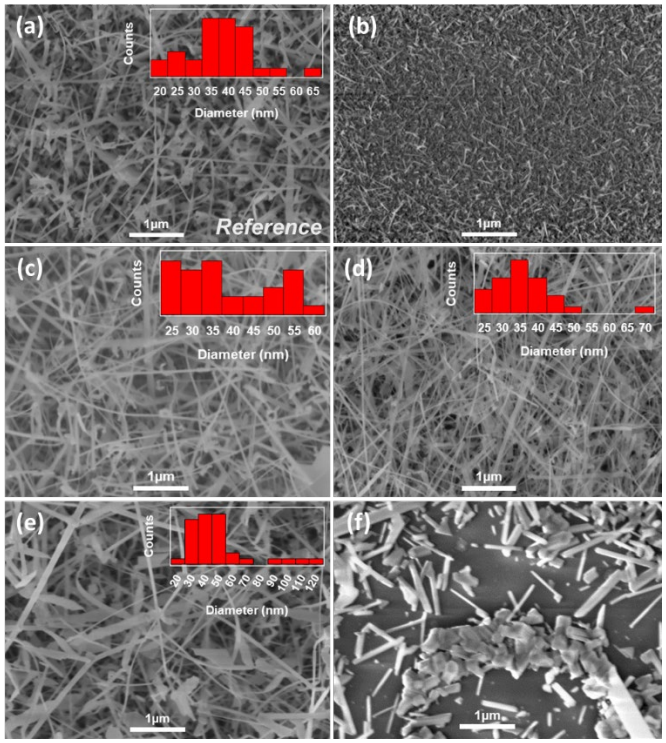

FIG. 3: It shows 6 samples of NWs grown at position 1 under different conditions. All NWs are grown as the (a) reference experiment but changing a condition: (b) 800°C, (c) 500 sccm, (d) 2000 sccm for the first 45 minutes of cooling, (e) 5 hours of growth and (f) Au-free substrate.

Other studies use the gas flow rate to tune the NWs, for instance, to make the diameter of the NWs larger by using a higher gas flow rate [12]. In this work, the morphology of NWs grown at 500 sccm is shown in Fig. 3c and, apparently, there are no differences in the morphology compared to the reference sample (grown at 2000 sccm). In addition, a reduced statistical study of the diameter of the NWs has been performed and its results are shown in the superimposed histograms of Fig. 3, indicating a diameter of ~20-65 nm.

The result of changing the flow, in comparison to the reference experiment, during the first 45 min of the cooling step to 2000 sccm is shown in Fig. 3d. As can be clearly seen, there is no obvious difference with the reference sample and the calculated diameter is in the same range.

By increasing the duration of the growth to 5 h, slightly thicker nanowires were obtained because of radial growth. This is illustrated in Fig. 3e, where NWs with a diameter up to ~115 nm can be seen. The fact that longitudinal growth is the preferred one, as it is catalysed by gold, does not exclude the radial growth.

Finally, the importance of Au as catalyst is demonstrated in Fig. 3f, corresponding to NWs grown without Au. A non-uniform layer of shorter NWs is obtained. An agglomeration of Ga_2O_3, in forms different from NWs, can also be seen. This is probably due to the self-catalysing properties of Ga_2O_3, but there is no control of the growth process.

B. Structural characterization

The grazing incidence XRD patterns of nanowires grown at different distances from the precursor are shown in Fig. 4. All diffraction peaks agree with the reference β-Ga_2O_3 (JCPDS card 00-041-1103) with monoclinic structure, C2/m space group, having lattice constants a = 1.22270 nm, b = 0.30389 nm, c = 0.58079 nm, α = 90.0000°, β = 103.8200° and γ = 90.0000°. No other crystalline phases of Ga_2O_3 were observed.

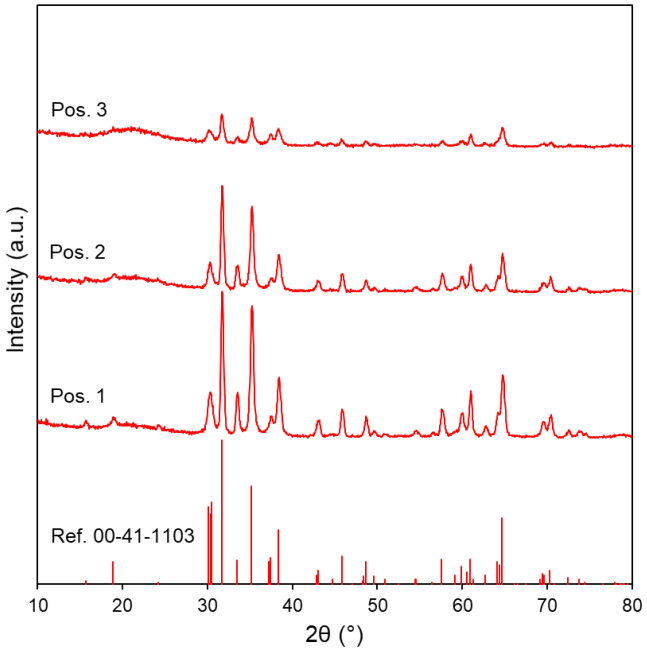

FIG. 4: XRD pattern for NWs grown at different distances from the evaporating source, together with the reference data for $\beta -Ga_2O_3$.

One can see that the relative intensities of the diffraction peaks are similar for these 3 samples but do not match the reference card. This is due to some preferred orientation of the NWs. In the 3 cases the most intense diffraction peak is located at 2θ ~ 31.7°, which corresponds to the (-202) crystal plane. However, analysing the relative intensities, one can see that the preferred orientation seems to be the (111), which corresponds to the peak at ~ 35.2°. Even though the nanowires grown at larger distances are shorter, the position of the diffraction peaks remains constant and, as a consequence, the lattice parameter does not change. In addition, the farther the nanowires have been grown from the precursor, the less intense the peaks, which can be associated to less amount of deposited material.

Around 2θ ~ 21-22°, a wide band is observed, which probably comes from the SiO_2 of the substrate.

Fig. 5 compares the XRD patterns of a sample grown on a Au-free substrate with another grown on a Au sputter-covered substrate. Both correspond to position 2 according to the notation in Fig. 1. In the Au-free sample, all diffraction peaks also match the reference pattern. However, in this case the most intense peak is located at 2θ ~ 35.2°, which corresponds to the (111) crystal plane. The absence of Au in the sample notably changes the preferred growth orientation of the nanowires.

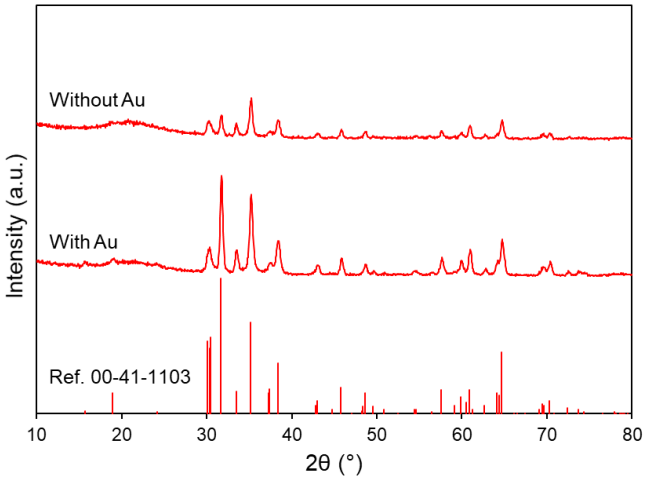

FIG. 5: XRD pattern for gallium oxide nanowires grown on different substrates, together with the reference data for monoclinic Ga_2O_3.

From the diffraction patterns, more information was extracted, as the peak broadening gives additional information about the sample microstructure. A well-known expression to estimate the crystallite size of nanophase materials from XRD peaks is the Scherrer equation:

$$\beta(2\theta) = \frac{K\lambda}{D\cos\theta} \qquad (1)$$

where β is the full width at half maximum of the peak, 2θ is the scattering angle in radians, λ is the wavelength, K is a constant, whose usual value is between 0.89 and 0.94, as a function of the fitted peak, and D is the dimension of the crystallites [13].

In this work, diffraction peaks have been fitted independently. Firstly, the background was stripped and then, each peak was fitted using a Gaussian-Lorentzian cross product function. For each pattern, three intense reflections, which do not overlap with others, were employed. Once the FWHM was obtained, the Scherrer equation (1) was used to approximate the crystalline size. The value of K has been taken as 0.9. These results (Table 1) are consistent with the SEM analysis: thicker nanowires were obtained by reducing the separation distance between metal source and substrate. However, the estimated size is different depending on the peak used because they correspond to crystalline domains in

different directions. The values are in agreement with the diameter of the NWs obtained from SEM.

Substrate	With Au				Au-free
Position	0	1	2	3	2
D at 31.7° (nm)	23.9	23.6	23.5	19.7	21.3
D at 35.2° (nm)	22.8	21.7	21.7	17.2	22.3
D at 38.4° (nm)	17.8	17.5	15.9	12.7	18.6

TABLE 1: Estimated crystalline sizes for different samples.

Some NWs were further investigated by TEM and their monocrystalline nature was confirmed. In the NW shown in Fig. 6, different interplanar spacings have been identified: ~0.127 nm, ~0.134 nm, ~0.145 nm and ~0.282 nm which corresponds to (-422), (-222), (-204) and (-202), respectively.

In addition, the NWs seemed to have a constant diameter and a very smooth surface. The NWs edges present a thin amorphous layer, whose thickness ranges from 0.5 to 1.5 nm around the NW. The EEL spectra, which were recorded while moving the electron beam across the section of the NW, confirmed that the edges also contain gallium and oxygen since no other signals were obtained. These signals are overlapped in Fig. 6, together with the carbon signal to demonstrate that no residual carbon is found. Therefore, it is confirmed that the NWs do not present carbon nor a core-shell structure, in opposition to the growth reported elsewhere [6].

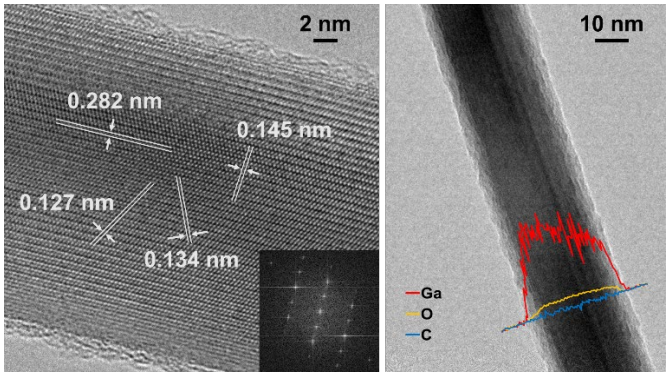

FIG. 6: (Left) High-resolution and (right) conventional TEM images of Ga_2O_3 nanowires grown at 900°C, 500 sccm and position 1. The inset of the left image is the calculated FFT.

C. Optical characterization

The bandgap of the grown Ga_2O_3 nanowires has been determined through UV-VIS spectrophotometry. Only one sample of NWs grown during 5 hours at 900°C and at ~7 cm from the precursor has been studied. Two transmittance measurements were made: one of the NWs grown on the substrate, $T_{NWs+Substrate}$, and one of the substrate prior to the growth, $T_{Substrate}$. In this way, by dividing them, we can obtain the transmittance of the NWs, T_{NWs}, which is shown in Fig. 7.

An absorption peak is observed at wavelengths close to 540 nm, which may be due to surface plasmon resonance (SPR) caused by the Au nanoparticles present in the sample, as it is reported that Au nanospheres with the size of 2–50 nm show only one plasmon band centred at about 520 nm [14]. This small discrepancy may have an explanation: microscopy images show that the Au droplets are not perfectly spherical for the grown NWs, in fact triangular shapes were also observed. The shape of the Au NPs determines the width, position, and number of SPRs [15].

The absorption coefficient of the NWs, α, can be calculated from this simple relation:

$$\alpha = \ln\left(\frac{1}{T_{NWs}}\right) = \ln\left(\frac{T_{Substrate}}{T_{NWs+Substrate}}\right) \qquad (2)$$

This has been used to determine the bandgap, E_g, using the Tauc relation which is given by this equation [16]:

$$(\alpha h\nu)^{1/\gamma} = B\left(h\nu - E_g\right) \qquad (3)$$

where h is the Planck's constant, ν is the frequency of the incident photons, B is a constant and γ is an index, which can be 2, 3, 1/2 or 1/3 corresponding to indirect allowed, indirect forbidden, direct allowed and direct forbidden transitions, respectively [17].

In this case, the best fitting was obtained by plotting $(\alpha h\nu)^2$ vs. $h\nu$, shown in Fig. 7, and fitting the linear part of the plot with equation (3) (red line). It was determined that the monoclinic Ga_2O_3 nanowires followed a direct allowed transition, with $\gamma = 1/2$, and the value of the bandgap, deduced as the crossing point of the red line with the x-axis, was found to be 4.70 ± 0.09 eV, which is in good agreement with the value reported in the Introduction section.

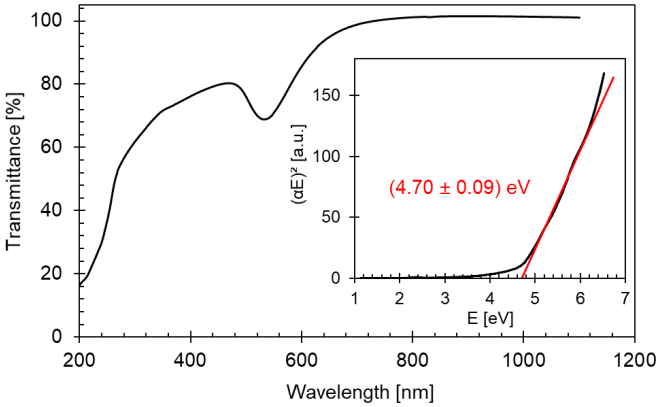

FIG. 7: Optical transmittance spectrum of Ga_2O_3 NWs. The inset shows the $(\alpha h\nu)^2$ vs. $h\nu$ plot (Tauc plot) used to determine the optical energy gap of the NWs.

IV. CONCLUSIONS

Monocrystalline β-Ga_2O_3 nanowires, with diameters between 13 and 115 nm and several micrometres long, have been successfully grown by CVD technique using gallium metal as a precursor.

Among the studied experiments, the optimal conditions for the growth of β-Ga_2O_3 NWs are maintaining source and substrate at 900°C and keeping them less than 3 cm apart. The use of Au as a catalyst is essential for the growth, while the use of a different gas flow rates has little impact. In addition, thicker nanowires were obtained by increasing the duration of the growth. The domain sizes estimated from XRD are consistent with the SEM analysis.

The light transmission spectra from one sample indicate that the NWs have a direct bandgap of about 4.70 eV, which agrees with the literature data.

V. ACKNOWLEDGMENTS

I sincerely acknowledge my advisor, Dr. Albert Romano, for his continuous support, patience and immense knowledge. He has given me the opportunity to enhance my background in applied physics by interpreting various measurements and using the knowledge acquired during my bachelor's degree, specifically in *Materials Physics*, *Solid State Physics* and *Micro and Nanotechnology* subjects.

This project could not have been accomplished without the assistance of Dr. Paolo Pellegrino and all the scientists from the CCiTUB, especially Dr. Luis López Conesa.

Last but not the least, I thank my family and friends for their constant encouragement during this period.

---

[1] A. Sharma, M. Varshney, H. Saraswat, «Nano-structured phases of gallium oxide (GaOOH, α-Ga_2O_3, β- Ga_2O_3, γ- Ga_2O_3, δ- Ga_2O_3, and ε- Ga_2O_3): fabrication, structural, and electronic structure investigations», *Int. Nano Lett.,* vol. 10, pp. 71–79, 2020. https://doi.org/10.1007/s40089-020-00295-w

[2] P.R. Jubu, F.K. Yam, O.S. Obaseki, Y. Yusof, «Synthesis and characterization of gallium oxide in strong reducing growth ambient by chemical vapor deposition», *Mater. Sci. Semicond. Process.*, vol. 121, 105361, 2021. https://doi.org/10.1016/j.mssp.2020.105361

[3] C. Jia, D.-W. Jeon, J. Xu, X. Yi, J.H. Park, Y. Zhang, «Catalyst-Assisted Large-Area Growth of Single-Crystal β-Ga_2O_3 Nanowires on Sapphire Substrates by Metal–Organic Chemical Vapor Deposition», *Nanomaterials*, vol. 10, 2020. https://doi.org/10.3390/nano10061031

[4] G. Domènech-Gil, «Advances in semiconducting nanowires for gas sensing: synthesis, device testing, integration and electronic nose fabrication», PhD Thesis, Universitat de Barcelona, 2019. http://hdl.handle.net/10803/668365

[5] G. Domènech-Gil, S. Barth, J. Samà, P. Pellegrino, I. Gràcia, C. Cané, A. Romano-Rodriguez, «Gas sensors based on individual indium oxide nanowire», *Sens. Actuators B Chem.*, vol. 238, pp. 447-454, 2017. https://doi.org/10.1016/j.snb.2016.07.084

[6] G. Domènech-Gil, I. Peiró, E. López-Aymerich, M. Moreno, P. Pellegrino, I. Gràcia, C. Cané, S. Barth, A. Romano-Rodriguez, «Room Temperature Humidity Sensor Based on Single β-Ga2O3 Nanowires», *Proceedings*, vol. 2, 2018. https://doi.org/10.3390/proceedings2130958

[7] J.D. Plummer, M.D. Deal, P.B. Griffin, Silicon VLSI technology: fundamentals, practice and modeling, pp 512–530, Pearson Education Inc, 2000.

[8] N.D. Cuong, Y.W. Park, S.G. Yoon, «Microstructural and electrical properties of Ga_2O_3 nanowires grown at various temperatures by vapor–liquid–solid technique», *Sens. Actuators B Chem.*, vol. 140, pp. 240-244, 2009. https://doi.org/10.1016/j.snb.2009.04.020

[9] R. E. Honig, H.O. Hook, «Vapor Pressure Data for Some Common Gases», *RCA Review*, vol. 21, p-360, 1960.

[10] R.S. Wagner, W.C. Ellis, «Vapor-liquid-solid mechanism of single crystal growth», *Appl. Phys. Lett.*, vol. 4, pp. 89-90, 1964. https://doi.org/10.1063/1.1753975

[11] E.I. Givargizov, «Fundamental aspects of VLS growth», *J. Cryst. Growth*, vol. 31, pp. 20-30, 1975. https://doi.org/10.1016/0022-0248(75)90105-0

[12] M. Kumar, V. Kumar, R. Singh, «Diameter Tuning of β-Ga_2O_3 Nanowires Using Chemical Vapor Deposition Technique», *Nanoscale Res. Lett.*, 12, 184, 2017. https://doi.org/10.1186/s11671-017-1915-1

[13] B. Ingham, M.F. Toney, «X-ray diffraction for characterizing metallic films», in Metallic Films for Electronic, Optical and Magnetic Applications, Ed: K. Barmak and K. Coffey, Woodhead Publishing, 2014.

[14] V. Amendola, «Surface plasmon resonance in gold nanoparticles: a review», *J. Phys. Condens. Matter*, vol. 29, 2017. https://doi.org/10.1088/1361-648X/aa60f3

[15] Y. Xia, N.J. Halas, «Shape-Controlled Synthesis and Surface Plasmonic Properties of Metallic Nanostructures», *MRS Bull.*, vol. 30, pp. 338–348, 2005. https://doi.org/10.1557/mrs2005.96

[16] J. Tauc, R. Grigorovici, A. Vancu, «Optical Properties And Electronic Structure of Amorphous Germanium», *Phys. Status Solidi B*, vol. 15, pp. 627-637, 1966. https://doi.org/10.1002/pssb.19660150224

[17] F. Urbach, «The Long-Wavelength Edge of Photographic Sensitivity and of the Electronic Absorption of Solids,» *Phys. Rev.*, vol. 92, p. 1324, 1953. https://doi.org/10.1103/PhysRev.92.1324